

## SENSITIVITY ANALYSIS ON THE BUILDINGS AND LANDSLIDES SEISMIC RESPONSE TO THE APPLICATION OF ARTIFICIAL AND RECORDED ACCELEROGRAMS

M.P. Boni<sup>1</sup>, M. Compagnoni<sup>1</sup>, C.G. Lai<sup>2</sup>, F. Pergalani<sup>1</sup>, L. Petrini<sup>1</sup>, V. Petrini<sup>1</sup>

<sup>1</sup> *Dipartimento di Ingegneria Strutturale - Politecnico di Milano, Piazza Leonardo da Vinci 32, 20133 Milano, Italy*

<sup>2</sup> *EUCENTRE, European Centre for Training and Research in Earthquake Engineering, Via Ferrata 1, Pavia*

### ABSTRACT :

In the paper the results of the dynamic analyses performed on landslides and buildings are presented. The aim of the project is the comparison of the influence due to the application of artificial and recorded accelerograms. So two different sets of artificial and recorded accelerograms have been applied on landslides and buildings. To have the accelerograms a probabilistic approach was adopted, on the basis of the data available from the Italian hazard map, for the studied site, two expected pseudo-acceleration elastic response spectra considering two return period (50 and 475 years) have been selected and used as target spectra. Starting from these targets two sets of seven artificial accelerograms have been calculated and two sets of seven recorded accelerograms have been selected from the available accelerogram database. To perform the dynamic analyses, in the first case (landslides) the method of Newmark has been used and the results, in term of expected displacements, are discussed. In the second case (buildings) the dynamic analyses have been performed using the "MIDAS Gen" software and the results, in term of storey base shear, acceleration and interstory drift are presented. The results, obtained by the application of the different sets of accelerograms, are similar, suggesting, in this kind of analysis, the possible use of both artificial and recorded accelerograms.

### KEYWORDS:

recorded accelerogram, artificial accelerogram, landslide, r.c. frame building, dynamic nonlinear time history analysis.

### 1. INTRODUCTION

To accurately evaluate the seismic behaviour of buildings and landslides it is necessary to use dynamic analyses. Obviously the choice of the seismic input is a fundamental step to perform a correct analysis. The seismic input can be expressed in term of artificial or recorded accelerograms. In both cases the accelerograms have to be well-matched with the expected pseudo-acceleration elastic response spectra of the studied site. In the case of recorded accelerograms, the choice is related to the knowledge of seismic characteristics of the site as the expected magnitude-distance combination, data not easily available. On the other hand, the characteristics of the artificial accelerograms (e.g. frequency content, duration, etc.) are strictly dependent on the generation methodologies and can be very different from the recorded ones. In some seismic codes the use of recorded accelerograms is suggested. In this paper, the results obtained by the application of both input types are discussed.

For the definition of the seismic input a probabilistic approach was adopted, because the studied site is located in a region where the seismic structures are still not very well known. Therefore, as it was impossible to separate the seismic hazard contribution coming from the possible sources, the cumulative contribution, on a probabilistic basis, was derived from all relevant neighbouring seismogenetic areas, which better represents an envelope of the expected seismic actions. On the basis of the data available from the Italian hazard map (Gruppo di Lavoro, 2004), for the studied site, two 5% damped pseudo-acceleration elastic response spectra, with return periods of 50 and 475 years, were selected and considered as target spectra. For each return period one sets of seven artificial and one sets of seven recorded accelerograms selected from available database were considered. These sets of inputs were used to perform dynamic analyses of different existing buildings and landslides.

### 1.1. Artificial accelerograms

Starting from each pseudo-acceleration elastic response spectrum of target (50 and 475 years) seven non-stationary accelerograms were generated through the procedure proposed by (Sabetta and Pugliese, 1996); the procedure is based on the Arias value (Arias, 1970) and the duration of the significant phase of the accelerogram: to obtain these parameters seven values of magnitude-distance couples, compatible with the expected maximum acceleration value, were chosen. In Figure 1 the uniform pseudo-acceleration elastic response spectrum of target and the response spectra of the computed artificial accelerograms, for the two return periods, are plotted. In the same Figure two accelerograms used in the analyses, for the two return periods, are presented.

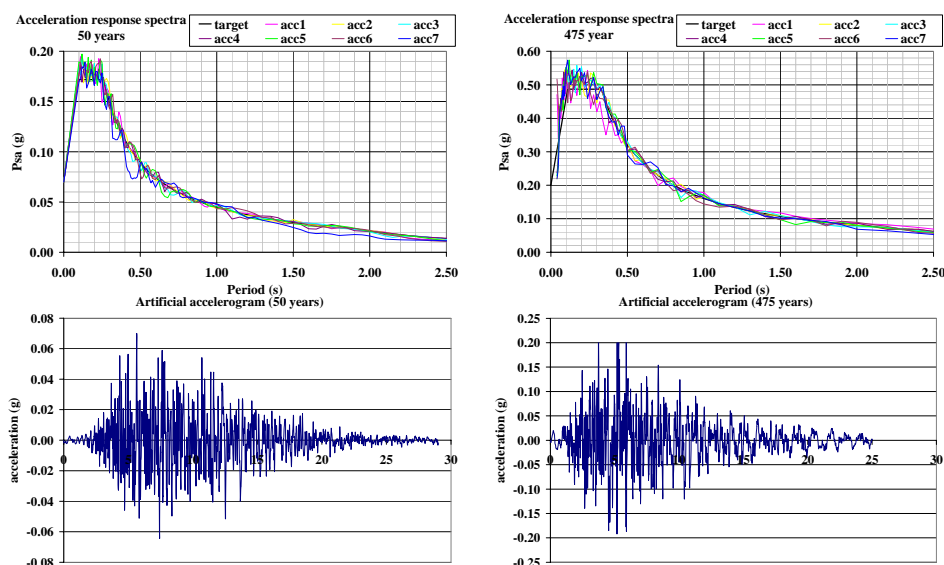


Figure 1. Response spectra and examples of artificial accelerograms

### 1.2. Recorded accelerograms

The recorded accelerograms were selected from strong motion record databases (ESD, PEER, COMOS), fixing the constraint of the spectrum compatibility with the target spectrum defined from the probabilistic seismic hazard assessment. The selection of the seven real spectrum-compatible accelerograms was conducted by using an algorithm (Dall'Ara et al., 2006) that automatically combines the records downloaded from the strong motion databases and identifies the best set that more reproduce the probabilistic response spectrum. The first criterion for the selection of real accelerograms is the geological characteristics of the site where the accelerometric station is installed. The site must be classified as a stiff soil site. Finally, the selected accelerograms were scaled to the target peak ground acceleration in order to have a good fitting of the mean response spectrum with respect to the probabilistic spectrum. A threshold of the scaling factor could be considered as further criterion of selection. In Figure 2 the uniform pseudo-acceleration elastic response spectrum of target, the response spectra of the recorded accelerograms and the average response spectrum of the recorded accelerograms, for the two return periods, are plotted. In the same Figure two accelerograms used in the analyses, for the two return periods, are presented.

In Table 1.1 the main characteristic parameters of the artificial and recorded accelerograms are reported:  $p_{ga}$ –peak ground acceleration,  $p_{gv}$ –peak ground velocity,  $si_{25}$ –spectral intensity (period 0.1-2.5 s, Housner, 1952),  $si_{05}$ –spectral intensity (period 0.1-0.5 s), a.i.–Arias intensity (arias, 1970),  $d_{90}$ –Trifunac duration (Trifunac and Brady,1975),  $T_{m90}$ –dominant period at  $d_{90}$ ,  $Pd_{90}$ –destructive potential (Saragoni et al., 1989) at  $d_{90}$ ,  $d_f$ –total duration,  $T_{mf}$ –dominant period at  $d_f$ ,  $Pd_f$ –destructive potential at  $d_f$ .

As shown in the Table the average of the characteristic parameters of the artificial and recorded accelerograms are similar, particularly considering the  $si_{25}$  and  $si_{05}$  parameters.

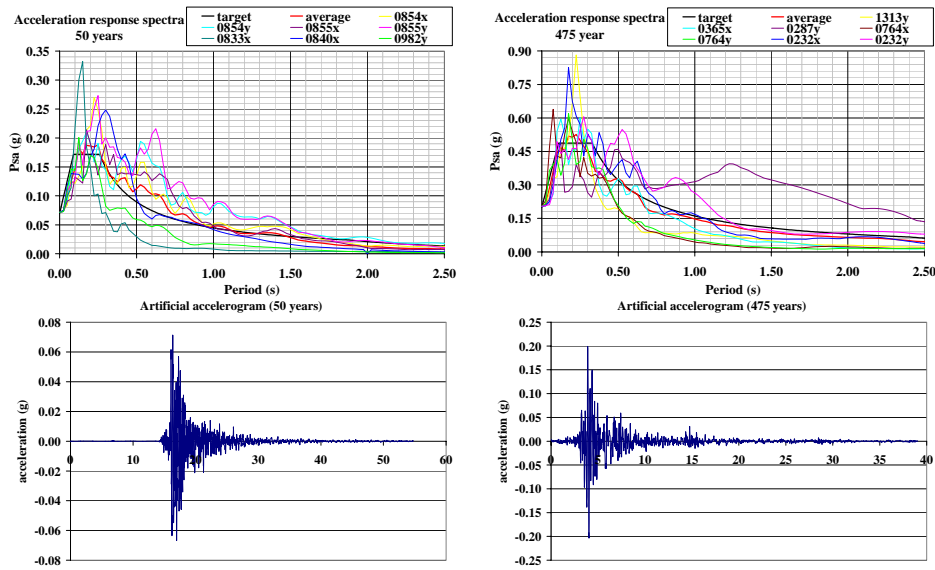


Figure 2 Response spectra and examples of recorded accelerograms

Table 1.1 Main characteristic parameters of the artificial (left) and recorded (right) accelerograms

	pga	pgv	si <sub>25</sub>	si <sub>05</sub>	a.i.	d <sub>0</sub>	Tm <sub>30</sub>	Pd <sub>30</sub>	d <sub>t</sub>	Tm <sub>y</sub>	Pd <sub>t</sub>		pga	pgv	si <sub>25</sub>	si <sub>05</sub>	a.i.	d <sub>0</sub>	Tm <sub>30</sub>	Pd <sub>30</sub>	d <sub>t</sub>	Tm <sub>y</sub>	Pd <sub>t</sub>	
	cm/s <sup>2</sup>	cm/s	cm	cm	cm/s	s	s	cm/s	s	s	cm/s		cm/s <sup>2</sup>	cm/s	cm	cm	cm/s	s	s	cm/s	s	s	cm/s	
acc1 50	68.65	-3.52	15.67	2.48	7.77	11.80	0.15	0.0445	29.00	0.15	0.0439		0854x	69.98	4.14	17.96	2.91	7.31	16.76	0.32	0.1825	72.73	0.30	0.1603
acc2 50	68.65	-3.70	15.83	2.51	7.34	10.86	0.16	0.0482	29.00	0.18	0.0577		0854y	69.98	4.57	22.98	2.90	7.11	16.31	0.36	0.2284	72.73	0.30	0.1586
acc3 50	-68.65	-3.82	15.68	2.45	7.36	12.34	0.14	0.0357	30.00	0.16	0.0476		0855x	-69.98	4.12	16.11	2.83	6.53	17.72	0.29	0.1401	72.74	0.29	0.1382
acc4 50	68.65	3.07	15.72	2.48	8.03	11.72	0.14	0.0373	30.00	0.15	0.0445		0855y	69.98	-4.91	23.53	3.31	9.67	16.33	0.33	0.2581	72.74	0.28	0.1850
acc5 50	68.65	3.92	15.59	2.50	7.93	12.38	0.15	0.0457	31.00	0.17	0.0548		0833x	69.98	1.82	3.81	1.45	3.10	4.17	0.15	0.0166	17.79	0.12	0.0103
acc6 50	-68.65	-3.21	15.62	2.50	6.94	13.62	0.15	0.0384	31.00	0.17	0.0484		0840x	69.98	-3.64	11.41	3.28	3.55	5.19	0.12	0.0121	54.74	0.25	0.0535
acc7 50	68.65	5.87	13.89	2.23	7.18	11.33	0.14	0.0360	32.00	0.17	0.0509		0982y	69.98	-2.04	5.85	1.78	1.49	3.07	0.16	0.0092	16.32	0.15	0.0082
average			15.43	2.45	7.51	12.01	0.15	0.0408	30.29	0.16	0.0497		average			14.52	2.64	5.54	11.36	0.25	0.1210	54.26	0.24	0.1020
acc1 475	196.13	16.04	60.21	7.55	60.88	13.16	0.16	0.4069	25.00	0.19	0.5501		1313y	-199.73	-10.62	27.98	6.68	19.38	4.37	0.17	0.1425	39.05	0.16	0.1267
acc2 475	-196.13	-15.38	58.17	8.12	67.12	12.20	0.15	0.4003	26.00	0.17	0.4661		0365x	199.73	-7.42	30.93	7.31	26.28	9.92	0.21	0.2928	30.67	0.21	0.3022
acc3 475	196.13	11.85	57.47	8.22	63.33	10.76	0.16	0.3966	26.00	0.16	0.4078		0287y	199.73	-28.78	127.76	6.47	50.62	31.78	0.25	0.8116	72.55	0.24	0.7113
acc4 475	196.13	-13.70	58.15	8.17	59.29	10.86	0.14	0.2950	26.00	0.15	0.3180		0764x	199.73	-9.04	20.22	6.55	51.36	9.34	0.08	0.0926	25.35	0.08	0.0859
acc5 475	196.13	13.01	56.97	8.28	61.94	12.18	0.14	0.3001	27.00	0.16	0.3794		0764y	-199.73	10.01	20.14	6.86	29.22	8.71	0.09	0.0648	25.35	0.09	0.0603
acc6 475	196.13	11.28	57.40	8.08	55.01	12.04	0.16	0.3743	28.00	0.18	0.4697		0232x	-199.73	12.16	49.77	8.81	50.04	11.65	0.21	0.5318	28.22	0.19	0.4706
acc7 475	-196.13	-14.67	55.77	8.13	67.25	11.36	0.17	0.4620	28.00	0.19	0.5781		0232y	199.73	-14.62	68.69	8.65	51.63	12.61	0.18	0.4309	28.22	0.20	0.5134
average			57.73	8.08	62.12	11.79	0.15	0.3765	26.57	0.17	0.4527		average			49.36	7.33	39.79	12.63	0.17	0.3381	35.63	0.17	0.3243

## 2. LANDSLIDES

### 2.1. Geologic, geomorphologic and geotechnical characteristics of the landslide

The analyzed landslide is characterized by alluvial deposits (debris and clay) on marls and limestones. It is a complex rotational slide (Figure 3), in particular the sector c is identified as an active landslide, instead the sectors a and b are classified as inactive landslides. The area of the entire landslide is 400.000 m<sup>2</sup>, the volume is 8 millions m<sup>3</sup>, the length is 1.080 m, the width is 590 m and the maximum depth is 50 m.

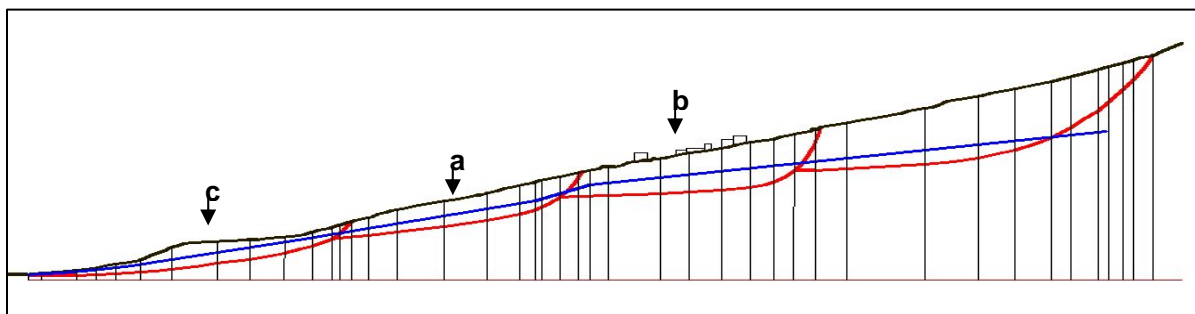


Figure 3 Representation of the analyzed landslide (blue line: water level, red line: failure surface)

Table 2.1 Geometric and geotechnical characteristics of the landslides

	V (m <sup>3</sup> )	M (t)	$\rho$ (t/m <sup>3</sup> )	$\phi$ (°)	$\alpha$ (°)
Entire landslide	24.347	48.450	1.99	17	10.0
a-b landslide	10.447	20.790	1.99	17	10.5
c landslide	2.980	5.930	1.99	17	11.0

On the basis of the geotechnical (11 bore-holes, 9 SPT tests, inclinometric and piezometric measures), geophysical (10 seismic refraction profiles) investigations and using the results of the laboratory tests (13 samples), the characteristics of the landslide materials, used in the analyses, have been obtained (Table 2.1 where V: volume, M: mass,  $\rho$ : density,  $\phi$ : friction angle,  $\alpha$ : failure surface angle).

## 2.2. Dynamic analysis method

The method used to determine the displacement of a landslide during an earthquake is the one proposed by Newmark (1965). This method calculates the response of a body, that stands on an inclined surface to a seismic acceleration acting at the base. It assumes the landslide is a rigid block with its own frictional properties at the surface-block boundary. The aim of the calculation is to determine the relative displacement induced by an earthquake of known characteristics and to estimate the stability of a mass during a seismic event. The base-block interface has a rigid-plastic behaviour and the resistance is expressed by the Mohr-Coulomb criterion. In the analysis it is assumed that if the limit resistance is exceeded a relative displacement between the base and the block may occur, representing the landslide. When the relative velocity becomes zero the block is again in contact with the base until the limit resistance is exceeded another time. This method can be applied on the whole landslide, after calculating the resultant of the resistant and acting forces. Displacement steps are summed up over the duration of the acceleration time history.

## 2.3. Results

The dynamic analyses, considering the accelerograms characterized by a return period of 475 years, were performed to the different sectors of the landslide, in particular the entire landslide, the a-b landslide and the c landslide. For each landslide a parametric analyses, considering three different level of the water table, was performed (saturation of 40%, 50% and 60%).

In Table 2.2 the results, in term of final displacements, are shown applying the artificial accelerograms and recorded accelerograms. In the Table the average final displacements, applying the different accelerograms, are reported.

Table 2.2 Displacements (m) applying the artificial (left) and recorded (right) accelerograms

Entire landslide									Entire landslide								
acc 1	acc 2	acc 3	acc 4	acc 5	acc 6	acc 7	average		1313y	0365x	0287y	0764x	0764y	0232x	0232y	average	
40%	0.027	0.032	0.029	0.024	0.027	0.025	0.034	0.028	40%	0.010	0.009	0.038	0.012	0.012	0.031	0.039	0.022
50%	0.059	0.059	0.058	0.050	0.058	0.046	0.067	0.057	50%	0.016	0.021	0.100	0.022	0.020	0.059	0.075	0.045
60%	0.127	0.120	0.124	0.113	0.121	0.105	0.134	0.121	60%	0.027	0.047	0.218	0.042	0.037	0.112	0.138	0.089
a-b landslide									a-b landslide								
acc 1	acc 2	acc 3	acc 4	acc 5	acc 6	acc 7	average		1313y	0365x	0287y	0764x	0764y	0232x	0232y	average	
40%	0.043	0.045	0.044	0.037	0.043	0.036	0.051	0.043	40%	0.013	0.016	0.069	0.017	0.016	0.045	0.056	0.033
50%	0.091	0.098	0.091	0.081	0.090	0.073	0.099	0.089	50%	0.022	0.033	0.159	0.032	0.029	0.085	0.107	0.067
60%	0.210	0.186	0.191	0.194	0.196	0.186	0.217	0.197	60%	0.040	0.077	0.341	0.066	0.055	0.165	0.209	0.136
c landslide									c landslide								
acc 1	acc 2	acc 3	acc 4	acc 5	acc 6	acc 7	average		1313y	0365x	0287y	0764x	0764y	0232x	0232y	average	
40%	0.067	0.066	0.066	0.057	0.066	0.052	0.074	0.064	40%	0.018	0.024	0.115	0.024	0.023	0.066	0.082	0.050
50%	0.146	0.135	0.140	0.130	0.139	0.122	0.153	0.138	50%	0.030	0.054	0.248	0.048	0.041	0.125	0.154	0.100
60%	0.372	0.324	0.348	0.336	0.343	0.379	0.346	0.350	60%	0.064	0.137	0.629	0.108	0.094	0.276	0.339	0.235

In Figures 4 and 5 the displacements vs. the time, for the artificial and recorded accelerograms respectively, are shown, considering the three analyzed landslides and the different water levels.

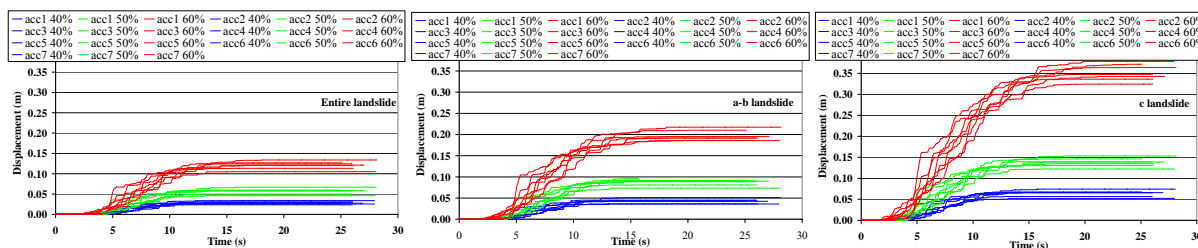


Figure 4 Displacement (m) behaviour applying the artificial accelerograms

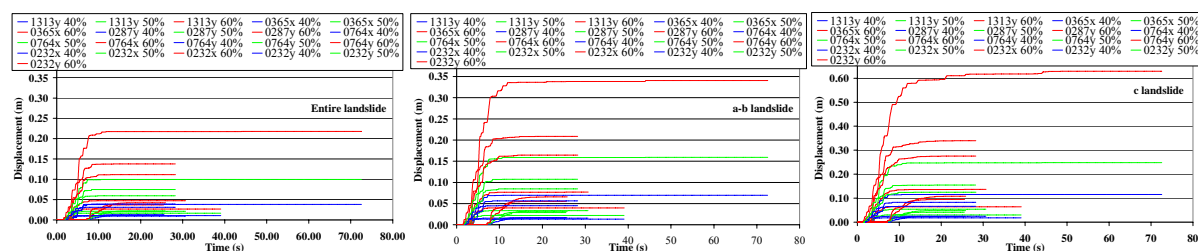


Figure 5 Displacement (m) behaviour applying the recorded accelerograms

As shown in the Figures, the c landslide presents the most dangerous situation, confirming the geomorphologic analysis (active landslide), instead the analysis performed considering the entire landslide gives the lowest displacements. The influence of the water level is fundamental, in fact the water levels at 50% and 60% produce displacements that can influence the stability of the buildings. Considering the results in term of average final displacements, it is noticed that the differences got applying the two sets of accelerograms (artificial and recorded) are not very high. In general the displacements obtained by the application of the recorded accelerograms are lower than the other one, probably due to the lower values, for some periods, of the average response spectrum of the recorded accelerograms with respect to the target spectrum.

The dynamic analyses, considering the accelerograms characterized by a return period of 50 years, were performed only on the c landslide, considering a saturation of 60%, because in the other cases the displacements are negligible. In Table 2.3 the results, in term of final displacements, are shown applying the artificial accelerograms and recorded accelerograms. In the Table the average final displacement, applying the different accelerograms, is reported. In Figure 6 the displacements vs. the time for the artificial and recorded accelerograms are shown. Also in this case the results in term of average final displacements applying the two sets of accelerograms (artificial and recorded) are similar.

Table 2.3 Displacements (m) applying the artificial recorded accelerograms

c landslide artificial accelerograms 50 years								c landslide recorded accelerograms 50 years									
acc 1	acc 2	acc 3	acc 4	acc 5	acc 6	acc 7	average	0854x	0854y	0855x	0855y	0833x	0840x	0982y	average		
60%	0.024	0.025	0.025	0.025	0.023	0.020	0.020	0.023	60%	0.037	0.043	0.039	0.058	0.006	0.017	0.003	0.029

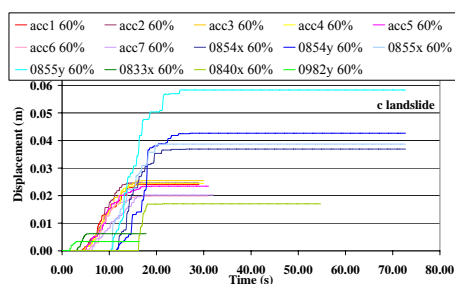


Figure. 6 Displacement (m) behaviour applying the artificial and recorded accelerograms

### 3. BUILDINGS

#### 3.1. Characteristics of the analysed buildings

The first building, designed according to the old Italian seismic code, is a three-storey r.c. frame building with masonry infill. The shape of the building (Figure 7) is roughly rectangular (33m x 10m). The frames are mono-directional and oriented parallel to the short sides. Concrete mean strength is  $f_{cm}=37\text{MPa}$  and steel mean yielding stress is  $f_{ym}=514\text{MPa}$  (Feb44k) for both longitudinal and transversal steel. The second building, designed without any seismic prescription, is a four-storey r.c. frame building with masonry infill. The shape of the building (Figure 8) is roughly rectangular (36m x 12.7m) with two r.c. cores. The frames are mainly mono-directional and oriented parallel to the long sides. Concrete strength is  $f_{cm}=37\text{MPa}$  and steel yielding stress is  $f_{ym}=514\text{MPa}$  (Feb44k) for both longitudinal and transversal steel.

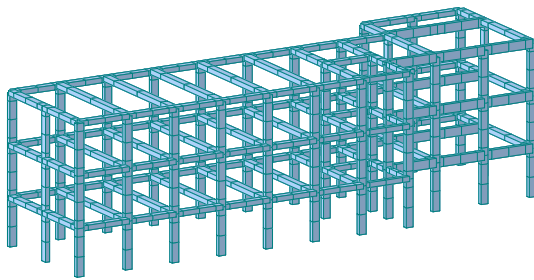


Figure 7 Building 1

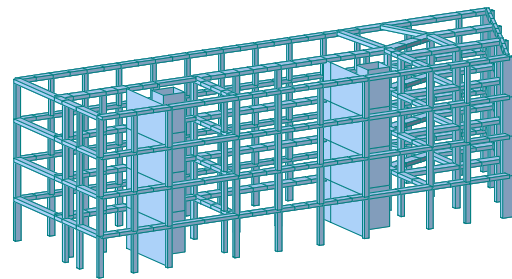


Figure 8 Building 2

#### 3.2. FEM models and dynamic analysis method

The nonlinear time-history dynamic analyses were developed through the software MIDAS Gen Ver. 721. The inelasticity in beams and columns was modeled with distributed plasticity fiber elements. The fiber constitutive models used for concrete and steel were the Kent and Park model (1971) extended by Scott et al. (1982) and the Menegotto and Pinto model (1973), respectively. The core walls of the second buildings were described using Shear-Wall elements included on the Finite Element Library of MIDAS program coupled with Drucker-Prager plasticity model (1952). Each floor was considered as a rigid diaphragm in its plane, and its mass was lumped at the centre of mass; hence for each floor only three degree of freedom were considered. The soil-structure interaction was neglected. The analyses were performed considering accelerograms acting in X and Y direction separately.

The implicit method of Newmark was adopted to integrate the equation of motion of the discrete system, performing full Newton-Raphson iterations until convergence was attained. In particular it was adopted a constant acceleration method, with the Newmark parameters  $\gamma=1/2$  and  $\beta=1/4$ . A viscous damping was adopted by defining the damping matrix as proportional both to the mass matrix and to the stiffness matrix and fixing at 5% the damping ratio for both the first and the second period of the structure.

#### 3.3. Results

For the comparison between the results obtained with the recorded and the artificial accelerograms the relative floor accelerations, the interstory drift ratio and the shear ratio were selected and reported for building 1 in Figures 9, 10 and 11, respectively. In all figures, the continuous lines refer to 475 years return period and dashed lines refer to 50 years return period. On the left are shown the results for accelerograms acting in the X and on the right the ones for accelerograms acting in the Y direction. For all the three considered quantities the differences between recorded and artificial accelerograms are very limited.

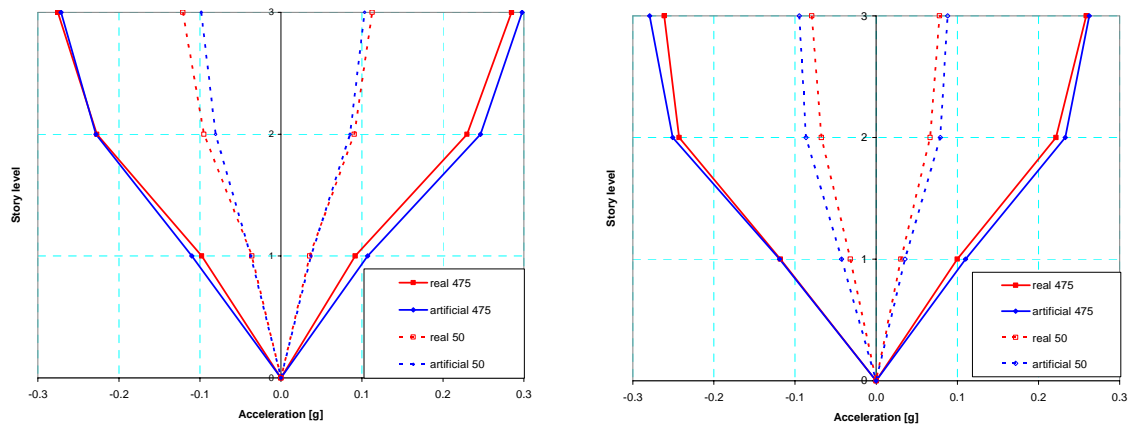


Figure 9 Building 1 - Story accelerations

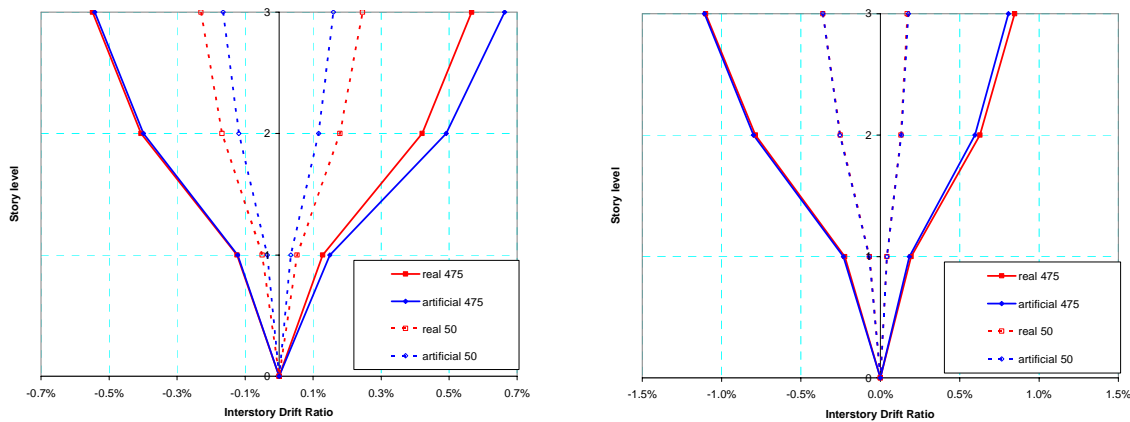


Figure 10 Building 1 - Interstory drift ratios

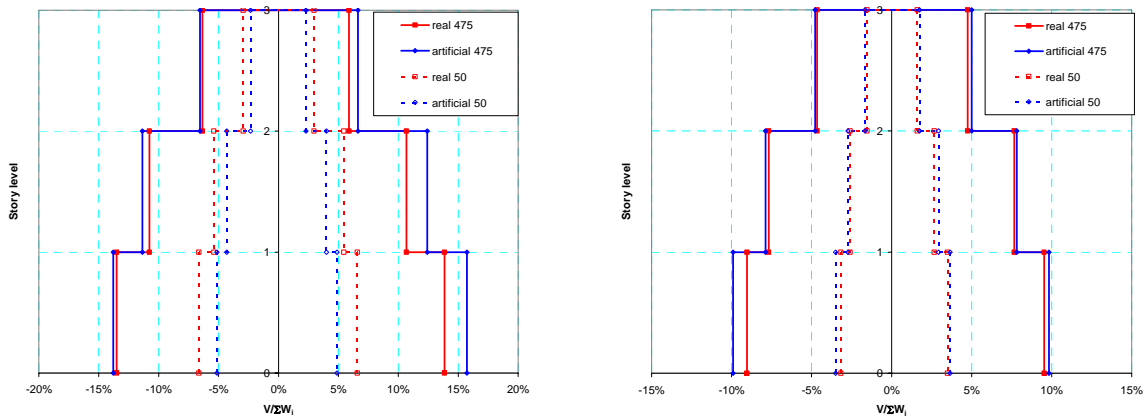


Figure 11 Building 1 - Shear ratio (story shear divided by the total weight of the building)

Similar results were obtained for building 2. As an examples in Figure 12, the shear ratio for the return periods of 50 and 475 years is shown: the left graph refers to the X direction and the right one refers to the Y direction.

#### 4 CONCLUSIONS

As a general conclusion, on the bases of the results obtained, it is possible to notice that the use of recorded and artificial accelerograms leads to similar results, on the average, both in the case of buildings and landslides. This is obviously a preliminary result: further analyses have to be performed considering different types of buildings and landslides. Moreover other criteria of generation and selection of accelerograms have to be investigated.

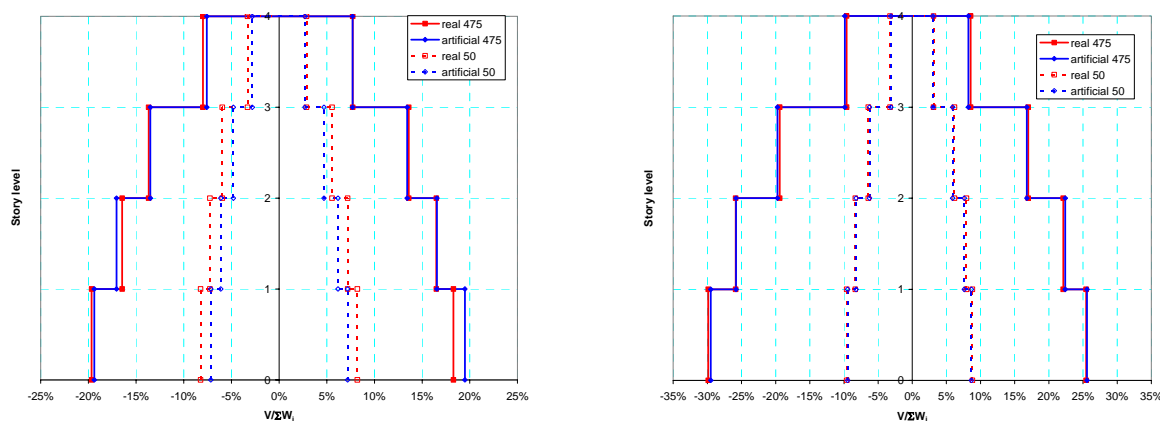


Figure 12 Building 2 - Shear ratio (story shear divided by the total weight of the building)

## ACKNOWLEDGMENTS

The authors would like to thank dr. Mirko Corigliano for the help in selecting the recorded accelerograms and Dr. Davide Spanò for the help in performing analyses.

## REFERENCES

- Arias, A. (1970). A measure of earthquake intensity. Seismic design for nuclear power plants, 1970. R.J.Hansen ed., Massachusetts Institute of Technology.
- COSMOS. Consortium of Organization for Strong Motion Observation Systems. <http://db.cosmos-eq.org/>.
- Dall'Ara, A., Lai, C. G. and Strobbia, C. (2006). Selection of spectrum-compatible real accelerograms for seismic response analyses of soil deposits. *Proceeding of First European Conference on Earthquake Engineering and Seismology*, Geneva, Switzerland, 3-8 September 2006.
- Drucker, D. C. and Prager, W. (1952). Soil mechanics and plastic analysis for limit design. *Quarterly of Applied Mathematics*. **10:2**, 157-165.
- ESD. European Strong Motion Database. <http://www.isesd.cv.ic.ac.uk/>.
- Gruppo di Lavoro 2004 (2004). Redazione della mappa di pericolosità sismica prevista dall'Ordinanza PCM 3274 del 20 marzo 2003. Rapporto conclusivo per il Dipartimento di Protezione Civile, INGV, Milano-Roma, 1-65.
- Housner, G.W. (1952). Spectrum Intensities of strong motion earthquakes. *Proceeding of the Symposium on Earthquakes and Blast Effects on Structures*. Earth. Eng. Res. Inst.
- Kent, D.C., Park, R. (1971). Flexural Members with Confined Concrete. *Journal of the Structural Division*, ASCE, 97 (ST7).
- Menegotto, M. and Pinto, P. E., (1973). Method of Analysis for Cyclically Loaded Reinforced Concrete Plane Frames Including Changes in Geometry and Non-Elastic Behavior of Elements under Combined Normal Force and Bending. *Proceedings, IABSE Symposium on Resistance and Ultimate Deformability of Structures Acted on by Well Defined Repeated Loads*, Lisbon, 15-22.
- MIDAS. Most Intelligent Design and Analysis System. Software solution for Structural Engineers. <http://www.midauter.com/>.
- Newmark, N.M. (1965). Effects of earthquake on dams and embankments, *Geotechnique* **23**.
- PEER. Pacific Earthquake Engineering Research Centre. <http://peer.berkeley.edu/smcat/>.
- Sabetta, F. and Pugliese, A. (1996). Estimation of response spectra and simulation of nonstationary earthquake ground motion. *Bull. Seism. Soc. Am.* **86:2**, 337-352.
- Saragoni, R., Holmberg, A. and Saez, A. (1989). Potencial destructivo y destructividad del terremoto del Chile de 1985. *Proceedings Sas. Jorn. Chilenas de Sismologia y Ing. Antisismica*, August 1989, **1** 369-378.
- Scott, B.D., Park, R. and Priestley, M.N.J. (1982). Stress-Strain Behavior of concrete Confined by Overlapping Hoops at Low and High Strain Rates. *ACI Journal* **79:1**, 13-27.
- Trifunac, M. D. and Brady, A. G. (1975). A study on the duration of strong ground motion. *Bull. Seism Soc. Am.* **65**.